Axonal transport of Frizzled5 by Alcadein α-containing vesicles is associated with kinesin-1

Yuzuha Shiraki[a], Monet Mitsuma[a], Ritsuko Takada[b,c], Saori Hata[a,d,i], Akira Kitamura[e,f], Shinji Takada[b,c], Masataka Kinjo[e], Hidenori Taru[a,i], Ulrike C. Müller[g], Tohru Yamamoto[h], Yuriko Sobu[a,i,j], and Toshiharu Suzuki[a,i,k,*]

[a]Laboratory of Neuroscience, Graduate School of Pharmaceutical Sciences, Hokkaido University, Sapporo 060-0812, Japan; [b]Exploratory Research Center on Life and Living Systems (ExCELLS), Okazaki, Aichi 444-8787, Japan; [c]National Institute for Basic Biology, National Institute of Natural Sciences, Okazaki, Aichi 444-8787, Japan; [d]Bioproduction Research Institute, National Institute of Advanced Industrial Science and Technology (AIST), Sapporo 062-8517, Japan; [e]Laboratory of Molecular Cell Dynamics, Faculty of Advanced Life Science, Hokkaido University, Sapporo 001-0021, Japan; [f]AMED-PRIME, Japan Agency for Medical Research and Development, 1-7-1 Otemachi, Chiyoda-ku, Tokyo 100-0004 Japan; [g]Institute of Pharmacy and Molecular Biotechnology, Im Neuenheimer Feld 364, 69120 Heidelberg, Germany; [h]Department of Molecular Neurobiology, Faculty of Medicine, Kagawa University, Miki-cho, Kagawa 761-0793, Japan; [i]Advanced Prevention and Research Laboratory for Dementia, Graduate School of Pharmaceutical Sciences, Hokkaido University, Sapporo 060-0812, Japan; [j]Laboratory of Neuronal Regeneration, Graduate School of Brain Science, Doshisha University, Kyotanabe 610-0394, Japan; [k]Department of Biological Sciences, Tokyo Metropolitan University, Tokyo 192-0397, Japan

ABSTRACT **Alcadein α (Alcα) and amyloid-β protein precursor (APP) are cargo receptors that associate vesicles with kinesin-1. These vesicles, which contain either Alcα or APP, transport various proteins/cargo molecules into axon nerve terminals. Here, we analyzed immune-isolated Alcα- and APP-containing vesicles of adult mouse brains with LC–MS/MS and identified proteins present in vesicles that contained either Alcα or APP. Among these proteins, Frizzled-5 (Fzd5), a Wnt receptor, was detected mainly in Alcα vesicles. Although colocalization ratios of Fzd5 with Alcα are low in the neurites of differentiating neurons by a low expression of Fzd5 in embryonic brains, the suppression of Alcα expression decreased the localization of Fzd5 in neurites of primary cultured neurons. Furthermore, Fzd5-EGFP expressed in primary cultured neurons was preferentially transported in axons with the transport velocities of Alcα vesicles. In synaptosomal fractions of adult-mice brains that express higher levels of Fzd5, the amount of Fzd5 and the phosphorylation level of calcium/calmodulin-dependent protein kinase-II were reduced in the Alcα-deficient mice. These results suggest that reduced transport of Fzd5 by Alcα-containing vesicles associated with kinesin-1 in axon terminals may impair the response to Wnt ligands in the noncanonical Ca^{2+}-dependent signal transduction pathway at nerve terminals of mature neurons.**

SIGNIFICANCE STATEMENT

- Alcadein α/Alcα is a cargo receptor that associates vesicles with kinesin-1.
- Alcα vesicles include characteristic proteins in adult brain neurons.
- Lack of Alcα impairs signal transduction at nerve terminals.

Monitoring Editor
Stephanie Gupton
University of North Carolina at Chapel Hill

Received: Nov 1, 2022
Revised: Aug 7, 2023
Accepted: Aug 10, 2023

This article was published online ahead of print in MBoC in Press (http://www.molbiolcell.org/cgi/doi/10.1091/mbc.E22-10-0495) on August 16, 2023.

*Address correspondence to: Toshiharu Suzuki (tsuzuki@pharm.hokudai.ac.jp).

Abbreviations used: Alcα, Alcadein α; APP, amyloid β-protein precursor; CaMKII, Ca^{2+}/calmodulin-dependent protein kinase II; EGFP, enhanced green fluorescent protein; Fzd, Frizzled; JIP, c-Jun NH2-terminal kinase (JNK)-interacting protein; KHC, kinesin heavy chain; KLC, kinesin light chain; SDC, sodium deoxycholate; SDS, sodium dodecyl sulfate; TIRF, total internal reflectance fluorescence.

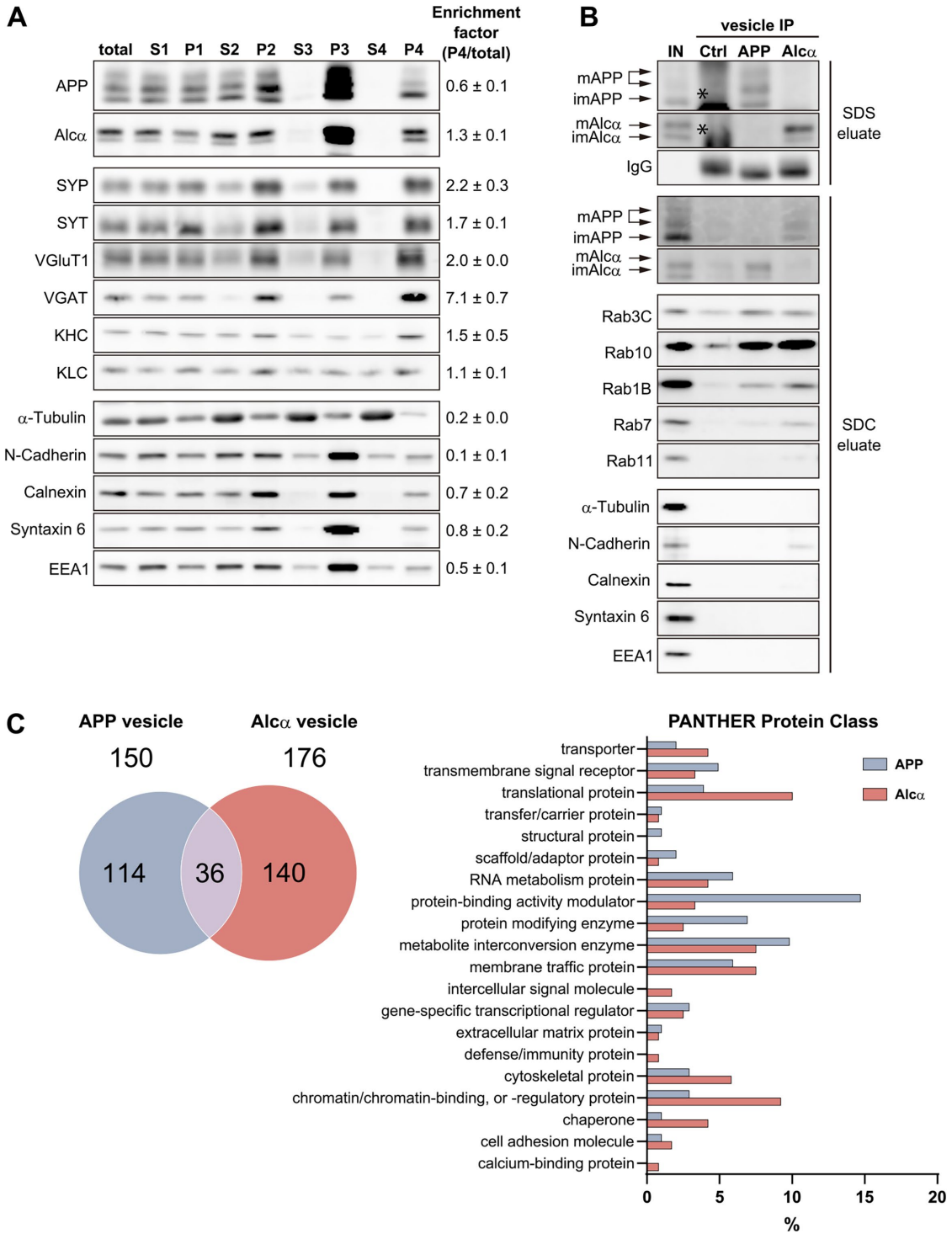

FIGURE 1: Preparation and characterization of Alcα- and APP-containing membrane vesicles, and identification of their protein content. (A) Characterization of the fractionated-membrane vesicles. Membrane vesicles of WT mice were prepared by fractionation using centrifugation, and proteins of respective fractions (10 μg protein/lane) were analyzed by immunoblotting with specific antibodies. The band density in the P4 fraction was compared with that in the brain homogenate (total) and indicated with a ratio (P4/total) for the enrichment factor. The values represent the average of three independent preparations ($n = 3$, mean ± S.E.), and the representative blot is shown. APP and Alcα are cargo receptors that connect the membrane vesicles with kinesin-1. SYP, SYT, VGluT1, and VGAT are proteins associated with membrane-transport vesicles. KHC and KLC are components of kinesin-1. α-Tubulin (cytosol), N-cadherin, calnexin (ER), syntaxin 6, and EEA1 are organelle marker proteins. (B) Characterization of Alcα- and APP-containing membrane-vesicle components. The P4 fraction in panel A (250 μg protein) was immunoprecipitated with anti-APP, anti-Alcα, and nonimmune IgG (Ctrl; 6 μg), and the proteins eluted with SDC and SDS solutions were analyzed by immunoblotting along with the P4 fraction before immunoprecipitation (IN, 5% protein amounts of the sample used for vesicular immunoprecipitation) for indicated proteins with specific antibodies. mAPP, mature APP (*N*- and *O*-glycosylated); imAPP,

INTRODUCTION

Alcadein (Alc) and amyloid β-protein precursor (APP) are type-I membrane proteins predominantly expressed in neurons (Araki *et al.*, 2003; Suzuki and Nakaya, 2008; van der Kant and Goldstein, 2015; Gotoh *et al.*, 2020). APP is the precursor of amyloid-β protein (Aβ), which is thought to give rise to the neurotoxic Aβ peptide in Alzheimer's disease (AD; Benilova *et al.*, 2012; Mucke and Selkoe, 2012). However, APP also has various physiological functions (Müller *et al.*, 2017; Richter *et al.*, 2018; Mehr *et al.*, 2020; Galanis *et al.*, 2021; Steubler *et al.*, 2021). Alcadein (Alc or calsyntenin/Clstn; Hintsch *et al.*, 2002) belongs to a small-gene family encompassing three proteins, Alcα/Clstn1, Alcβ/Clstn3, and Alcγ/Clstn2, all of which are subject to proteolytic cleavage by the same secretases as APP (Araki *et al.*, 2003; Hata *et al.*, 2009; Piao *et al.*, 2013). These Alcs form a tripartite complex with APP through a process mediated by a cytoplasmic neuronal adapter protein X11-like (X11L), which stabilizes the metabolism of both APP and Alcs (Araki *et al.*, 2004; Kondo *et al.*, 2010; Motodate *et al.*, 2016). Among the Alcs, Alcα, and Alcβ are thought to be associated with AD pathophysiology (Araki *et al.*, 2003, 2004; Hata *et al.*, 2009, 2011; Omori *et al.*, 2014). Alcα-KO mice facilitate the development of amyloid pathology in human APP transgenic AD model mice (Gotoh *et al.*, 2020), and Alcβ modulates AD progression (Hata *et al.*, 2019; Gandy, 2023; Hata *et al.*, 2023).

Both Alcα and APP are known to serve as receptors of membrane-transport vesicles that link their vesicle cargo with kinesin-1, either directly or indirectly (Konecna *et al.*, 2006; Araki *et al.*, 2007). Therefore, Alcα and APP are referred to as kinesin-1-dependent cargo receptors that are important to preserve neuronal functions. Kinesin-1 is the first anterograde-molecular motor to be identified in the neuronal axon (Vale *et al.*, 1985) and is composed of two kinesin heavy chains (KHC/KIF5) and two kinesin light chains (KLC) (reviewed in Verhey and Hammond, 2009). Kinesin-1 is thought to play an important role in the long-distance transport of membrane vesicles and organelles, especially in neurons. Two KLC-binding tryptophan- and aspartic acid-containing (WD) motifs in the cytoplasmic domain of Alcα directly associate with the tetratricopeptide repeat (TPR) motifs of KLC (Araki *et al.*, 2007; Dodding *et al.*, 2011), which activates kinesin-1 from an autoinhibitory state and triggers the transport of Alcα-containing membrane vesicles (Kawano *et al.*, 2012; Zhu *et al.*, 2012; Yip *et al.*, 2016). The interaction between WD motifs and KLC is regulated by the phosphorylation of multiple sites within an acidic region of Alcα. The phosphorylation of the acidic region located between two WD motifs is essential for Alcα vesicle formation at the Golgi exit zone (Sobu *et al.*, 2017).

APP is also a cargo receptor of membrane-transport vesicles via its association with kinesin-1 (Kamal *et al.*, 2000; Araki *et al.*, 2007; Chiba *et al.*, 2014a). APP is linked to kinesin-1 via the JNK-interacting protein 1 (JIP1) leading to enhanced fast velocity (EVF) of APP membrane vesicle transport in the neuronal axon (Szodorai *et al.*, 2009; Chiba *et al.*, 2014a; Chiba *et al.*, 2017; Tsukamoto *et al.*, 2018). This association between APP and kinesin-1, mediated by the JIP1b isoform, is regulated by the complex interaction between JIP1b and KLC1 (Verhey *et al.*, 2001; Chiba *et al.*, 2014a). This interaction that generates a particularly fast velocity, in which the vesicles are transported faster than the speed at which kinesin-1 moves on microtubule in vitro, is regulated by the phosphorylation of KLC1 (Chiba *et al.*, 2017). Interestingly, APP-containing membrane transport vesicles are distinguished from Alcα-containing membrane transport vesicles mainly through their axonal-transport velocities in neurons in vitro (Araki *et al.*, 2007; Chiba *et al.*, 2014a), suggesting that they each transport distinct cargos/contents in their vesicles. However, it remains unclear what types of cargo proteins are transported in Alcα and/or APP vesicles associated with kinesin-1, and what functions these cargo proteins are performing at nerve terminals.

To reveal specific and/or common cargo proteins within APP- and Alcα-transport vesicles and to understand the function of these cargo proteins at the nerve terminals of mature neurons in adult brains, we isolated APP- and Alcα-containing vesicles from adult-mouse brains using specific antibodies and analyzed proteins associated with/or included in both transport vesicles. We revealed that Alcα-transport vesicles included characteristic cargo proteins, which are largely different from cargo proteins included in APP-transport vesicles in adult brains. We focused on Fzd5, one of these cargo proteins of Alcα-transport vesicles, and analyzed the transport of Fzd5 in axons of primary culture neurons. Transport of Fzd5 by Alcα-transport vesicles was not exclusive in the immature neurons, which differs from mature neurons in the adult brains. However, the exogenously expressed Fzd5-EGFP was transported with the velocity of Alcα vesicles rather than that of APP vesicles in the axon of immature neurons. These observations suggest that the cargo selectivity of cargo proteins may be completed after neuronal maturation. Furthermore, we propose the possible functions of Fzd5 at nerve terminals of mature neurons in adult-mouse brains. We detected that the activation of Ca^{2+}/calmodulin-dependent protein kinase-II, a noncanonical signal-transduction pathway by Wnt, was impaired in the brain-synaptosomal fraction of Alcα-deficient mice. This may be due to insufficient Fzd5 transport in the absence of Alcα-transporting vesicles. We show the importance of cargo receptors of long-driving kinesin-1 motors such as Alcα and APP in the localization of cargo proteins at nerve termini which may in turn be crucial for signal transduction.

RESULTS

Alcα- and APP-transport membrane vesicles contain distinct cargo contents

To isolate Alcα- and APP-containing vesicles, we prepared a membrane vesicle fraction (P4 fraction) with a yield of ~0.8% protein of total brain lysate from wild-type (WT) mice. The vesicular size in the P4 fraction was mostly smaller than ~200 nm in diameter as observed with Scanning Transmission Electron Microscopy (STEM) following negative staining of the sample (Supplemental Figure S1). To characterize the vesicles, we used immunoblotting to analyze the protein components of the vesicles (Figure 1). The P4 fraction was enriched in proteins related to vesicular trafficking (synaptophysin

immature APP (*N*-glycosylated); mAlcα, mature Alcα (complex *N*-glycosylated); imAlcα, immature Alcα (high mannose *N*-glycosylated). Asterisk (in Ctrl) indicates a nonspecific product. The enrichment factors of Rab proteins are shown in Supplemental Figure S2. (A, B) Molecular size markers are indicated in Supplemental Figure S2. (C) Classification of proteins identified within APP- and Alcα- transport vesicles. SDC eluates of APP- and Alcα-containing vesicles were analyzed by LC-MS/MS analysis as shown in the Venn diagram (left). The identified proteins were classified based on PANTHER Protein Class (right). Proteins identified by five independent analyses with LC–MS/MS are described (Supplemental Tables S1–3 and Supplemental Data1).

[SYP], synaptotagmin [SYT], vesicular glutamate transporter 1 [VGluT1], and vesicular GABA transporter [VGAT] together with kinesin-1 components KHC and KLC), compared with cytosolic (α-tubulin) and organelle marker proteins (plasma membrane [N-cadherin], endoplasmic reticulum/ER [calnexin], *trans*-Golgi network/TGN [Syntaxin 6], and early endosome [EEA1]; Figure 1A). The cargo-receptor molecules APP and Alcα were also recovered in the P4 fraction and within P3 fraction, which mainly includes the larger membrane-bound organelles such as endosomes, Golgi apparatus, and ER, to where APP and Alcα are mostly localized.

Using antibodies specific to the cytoplasmic region of Alcα and APP and nonimmune IgG (control/Ctrl), Alcα- and APP-containing membrane vesicles were isolated from the P4 fraction, and their membrane cargo contents were eluted first with SDC and then with SDS to recover the membrane-associated IgG-bound cargo receptors (Figure 1B). The membrane vesicles recovered with the Alcα antibody include largely mature Alcα (mAlcα), which possesses complex *N*-glycosylation (Araki *et al.*, 2007), in SDS eluate. Similarly, membrane vesicles recovered with the APP antibody include predominantly mature APP695 (mAPP) species, which are *N*- and *O*-glycosylated forms in neurons (Suzuki and Nakaya, 2008). These mature forms are found in vesicles in the late secretory pathway. Furthermore, in SDC eluate, both Alcα and APP vesicles were associated more with Rab3 and Rab10, which are involved in vesicular transport from the TGN, than with other Rab proteins. Rab1 regulates transport to the Golgi apparatus from the ER, Rab7 controls transport to lysosomes from late endosomes, and Rab11 regulates the transport around recycling endosomes (see Figure 1B and Supplemental Figure S2B for the enrichment factor of Rab proteins; Kjos *et al.*, 2018). Other cytoplasmic (α-tubulin) and organelle markers (N-cadherin, calnexin, syntaxin6, and EEA1) proteins are excluded. Taken together, these analyses indicate that membrane vesicles, after exiting the Golgi apparatus, were recovered by immunoprecipitation. Alcα-harboring vesicles contained some APP and vice versa for APP vesicles (faintly detected in the SDC eluate, Figure 1B), which agrees with previous observations that almost 30% of Alcα-containing vesicles colocalize with APP in the axon of sciatic nerves of adult mice (Araki *et al.*, 2007).

Samples eluted with SDC were analyzed with LC–MS/MS and listed with gene/protein names, accession numbers, the number of unique peptides, and sequence coverage (Supplemental Tables S1, proteins detected in APP-containing vesicles; S2, proteins detected in Alcα-containing vesicles; S3, proteins detected in both APP- and Alcα-containing vesicles). Numbers and types of proteins detected in respective Alcα- and APP-harboring vesicles are summarized in Figure 1C. Proteins detected by immunoprecipitation with nonimmune IgG were excluded, and we finally identified 176 proteins from Alcα-containing vesicles and 150 proteins from APP-containing vesicles, with 36 proteins present in both vesicle subtypes. We classified these proteins using the PANTHER (Protein analysis through evolutionary relationship) Protein Classification system (Thomas *et al.*, 2022). With the exception of proteins such as "translational proteins," which mostly function in the cell body, APP-containing vesicles associate with proteins that are "protein-binding activity modulators", "protein modifying enzymes", and "metabolite interconversion enzymes". However, Alcα-containing vesicles preferentially associate with "cytoskeletal proteins", "chaperones", and "cell adhesion molecules" (Figure 1C). Interestingly, both vesicles included moderate levels of "transmembrane signal receptors". For example, Ephrin type-A receptor 10, IGF-like family receptor one, and Glycoprotein M6B were included in APP-containing vesicles, whereas Frizzled-5 (Fzd5), Netrin receptor A Unc-5, and Sortilin were characteristically detected in Alcα-harboring vesicles. Among these proteins that are possibly associated with Alcα- and APP-containing membrane vesicles, we first focused on Fzd5 for further analysis. This was because some phenotypes observed in Alcα-deficient animals, such as aberrancies within axonal guidance and synapse formation, are likely to be involved in Fzd5 function (Sahores *et al.*, 2010; Slater *et al.*, 2013; Ortiz-Medina *et al.*, 2015; Alther *et al.*, 2016) and Wnt signaling (Inestrosa and Varela-Nallar, 2015).

Fzd5 is predominantly found in Alcα-containing vesicles of adult-mouse brains

We examined in which vesicles, Alcα- or APP-containing transport vesicles of adult-mouse brains, Fzd5 is detectable using immunoblotting and immunostaining (Figure 2). Proteins eluted from Alcα- and APP-harboring vesicles with SDC were analyzed by immunoblotting with an anti-Fzd5 antibody and with antibodies against marker proteins. Immune-isolated vesicles were then further solubilized in SDS to confirm the presence of IgG-associated cargo receptors, Alcα and APP. Compared with other proteins involved in vesicular transport, such as VGAT, SYT, and SYP; Fzd5 was yielded more (more than six-fold) in Alcα- than in APP-containing vesicles (Figure 2A). We further confirmed that Fzd5 was present in vesicles transported by kinesin-1. The P4 fraction was subjected to immunoisolation with an anti-KHC antibody, and the contents of isolated vesicles were analyzed by immunoblotting (Figure 2B). The anti-KHC antibody recovered Alcα and APP, kinesin-1 cargo receptors, along with KLC, and further yielded Fzd5 together with VAMP2 and SYP. These results strongly indicate that transporting vesicles associated with kinesin-1 contain Fzd5 together with their cargo receptors. This biochemical analysis indicates that Fzd5 is contained within Alcα-containing vesicles in higher abundance than in APP-containing vesicles and is transported by kinesin-1 motor proteins.

Next, we examined the colocalization of Fzd5 with Alcα or APP in axons of differentiating neurons. Mouse primary cultured neurons (DIV 4–5) were immunostained with antibodies against APP, Alcα, and Fzd5. Vesicles in which axonal Fzd5 colocalized with Alcα or APP were shown with the colocalization efficiency (Figure 2C). The colocalization rates of Fzd5 with Alcα and APP indicated as Pearson's *R*-value were lower, which does not agree with the biochemical analyses of adult-mouse brains (Figures 1 and 2, A and B). Although Fzd5 colocalized with Alcα with higher rates than APP ($p < 0.01$; Figure 2C, right graph), the results indicate that the majority of Alcα and APP vesicles do not include Fzd5 in axons of primary cultured neurons. We examined the levels of Fzd5 expression in the brain during postnatal day 0 to 6-mo-old (Figure 2D). The expression levels of Fzd5 were very low until postnatal day 7, which agreed with a previous report that the brain expression of Fzd5 was extremely low during embryonic days to postnatal day 10 (Slater *et al.*, 2013). The previous literature and our result indicate that the expression of Fzd5 is very low in immature neurons that we used here when compared with the expression level of Fzd5 in adult-mouse brains that we analyzed biochemically. This may be a reason for lower colocalization rates of Fzd5 with Alcα in the axon of the primary cultured neurons. Small amounts of Fzd5 expressed in immature neurons may be concentrated into restricted transporting vesicles in the axon.

To confirm that Alcα vesicles transport Fzd5 in primary cultured neurons, we examined whether the reduced expression of Alcα decreases Fzd5 distribution in axons (Figure 3). Alcα in mouse primary cultured neurons reduced by the expression of shRNA against Alcα. Alcα immunostaining in the cell body decreased by ~50% compared with in mock-treated cells (Figure 3A). In a separate study, APP

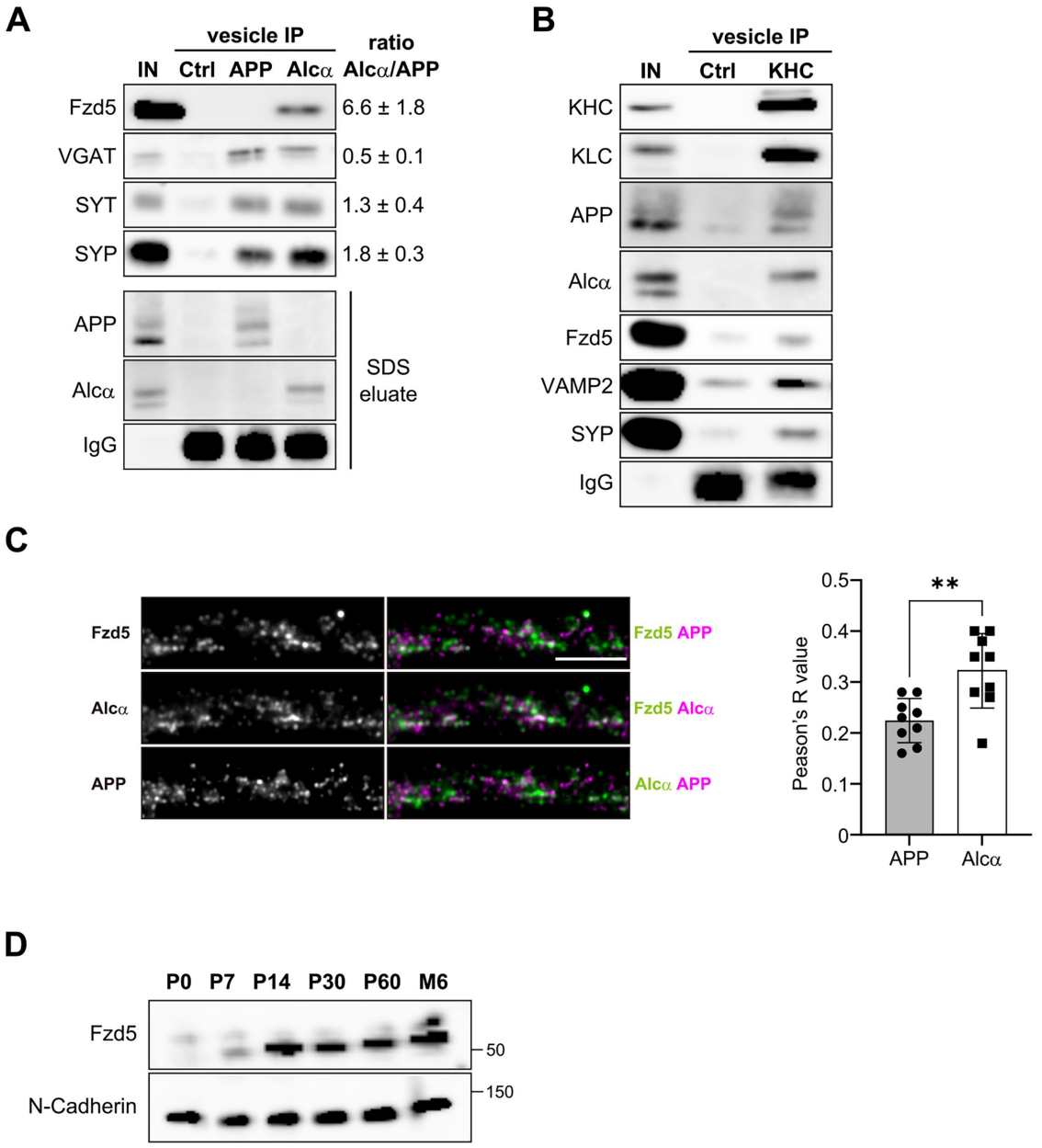

FIGURE 2: Fzd5 in Alcα- and APP-containing membrane vesicles and colocalization with Alcα and APP in axons. (A) Fzd5 in Alcα- and APP-harboring vesicles. Alcα- and APP-containing vesicles isolated with their antibodies were analyzed together with control nonimmune IgG (Ctrl) by immunoblotting for the proteins indicated; Fzd5, VGAT, SYT, SYP. Protein ratios in Alcα vesicles to APP vesicles are shown (Alcα/APP). The values are the average of three independent preparations ($n = 3$, mean ± S.E.), and the representative immunoblot is shown. The presence of Alcα and APP in their respective vesicles was confirmed by immunoblot analysis of SDS eluate. (B) Contents of vesicles isolated with a KHC antibody against kinesin-1. The P4 fraction in Figure 1A (250 μg proteins) was subjected to vesicle immunoprecipitation with an anti-KHC antibody (KHC) or nonimmune IgG (Ctrl) and analyzed by immunoblotting for indicated proteins. In panels A and B, IN indicates the analysis with 5% protein of the sample used for vesicle immunoprecipitation. (A, B) Molecular-size markers are indicated in Supplemental Figure S3. (C) Colocalization of Fzd5 with Alcα and APP in a mouse-neuronal axon. Primary cultured mouse neurons (DIV 4–5) were immunostained triply with anti-Fzd5, anti-Alcα, and anti-APP antibodies, and axonal stainings are shown. Scale bar, 2 μm. Colocalization efficiency of Fzd5 with Alcα or APP was calculated using Coloc2 plugin. The colocalization rates were calculated from each frame of images of axons and are indicated as Person's *R* value in the right panels (*R* value of 1.0 indicates perfect colocalization while an *R* value of 0 indicates random localization). Asterisk (**) indicates $p < 0.01$ ($n = 7$ [cell number], mean ± S.E.). Statistical analyses were assessed using Student's *t* test (left graph). (D) Expression of Fzd5 in the brain of postnatal stages. The brain lysates (10 μg protein) of the indicated postnatal stages of WT mice were analyzed by immunoblotting with anti-Fzd5 and anti-N-cadherin antibodies. P0, postnatal 0 day; P7, postnatal 7 day; P14, postnatal 14 day; P30, postnatal 30 day; M6, 6-mo-old. Molecular size markers (kDa) are indicated on the right side.

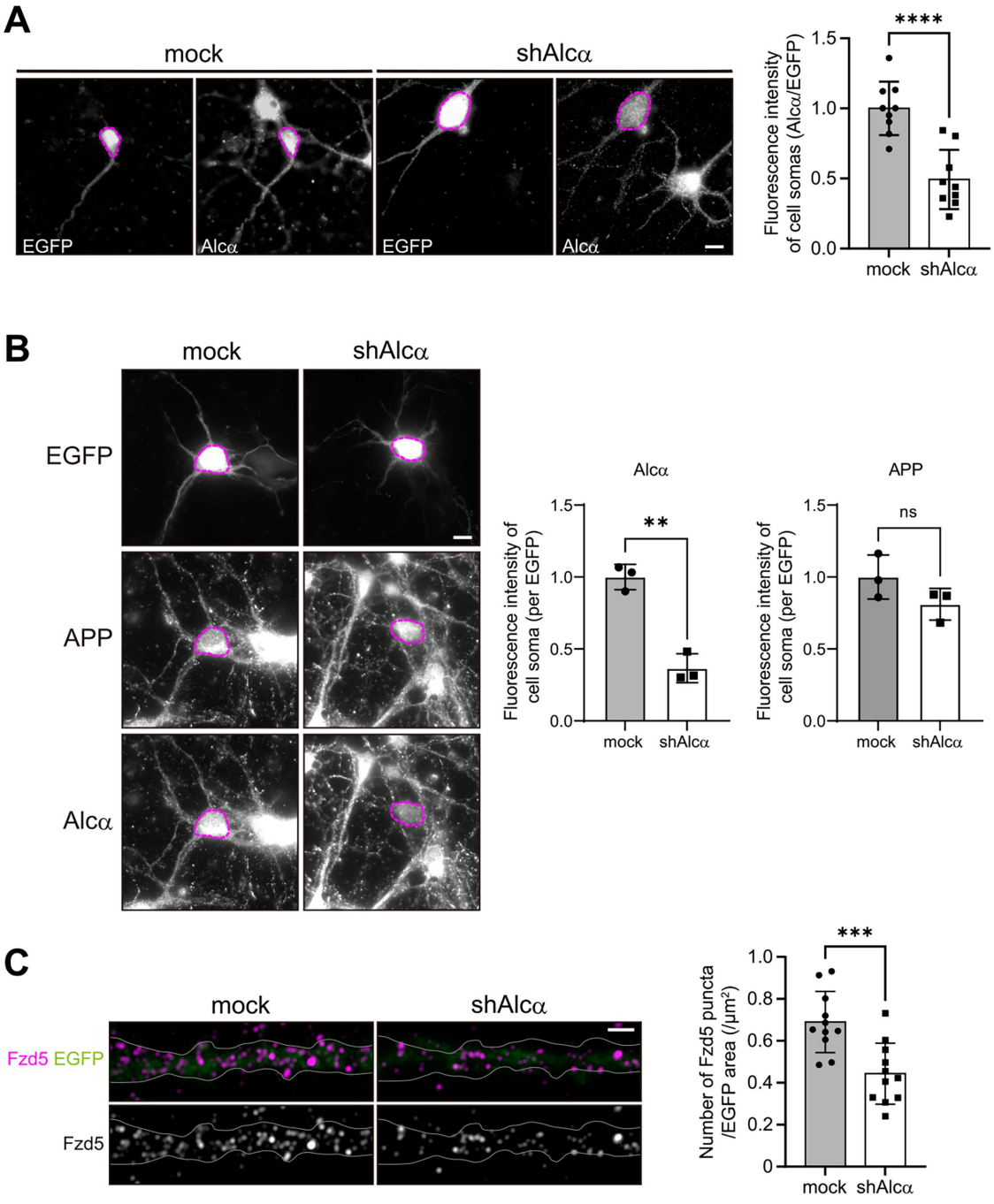

FIGURE 3: Decreased Fzd5 levels in neuronal axons by suppressing Alcα expression. (A) Reduced expression of Alcα in mouse neurons with shRNA against Alcα. Mouse-primary cultured neurons (DIV 4–5) were transfected with shRNA vectors against Alcα or control (mock) along with EGFP. Endogenous Alcα expression was examined by immunostaining. Alcα signals in EGFP-expressing areas (enclosed by a magenta line) were quantified and standardized with EGFP fluorescence. Scale bar, 10 μm. The fluorescence intensity of neurons treated with shRNA was compared with that of mock-treated neurons assigned at 1.0. Asterisks (****) indicate $p < 0.0001$ ($n = 11$ [cell number], mean ± S.E.). Statistical analyses were assessed using Student's *t* test. (B) Preserved expression of APP in mouse neurons with shRNA against Alcα. Neurons transfected with shRNA vector against Alcα with EGFP were immunostained with APP- and Alcα antibodies. The fluorescence intensities of APP and Alcα in neurons transfected with shRNA were compared with those in neurons transfected with a mock vector. APP and Alcα signals in EGFP-expressing areas (enclosed by a magenta line) were quantified and standardized with EGFP fluorescence. Scale bar, 10 μm. The fluorescence intensity of APP and Alcα of neurons treated with shRNA was compared with that of mock-treated neurons assigned at 1.0. Asterisks (**) indicate $p < 0.01$ ($n = 3$ [cell number], mean ± S.E.). Statistical analyses were assessed using Student's *t* test (ns, not significant). (C) Reduced Fzd5 expression in neuronal axons treated with shRNA against Alcα. Fzd5-positive signals (magenta) in the axons of neurons are shown (left). Scale bar, 2 μm. The numbers of Fzd5-positive bright spots in axons exposed to shRNA in EGFP-expressing areas (green) were counted and compared with those of mock-treated neurons (right graph). Asterisks (***) indicate $p < 0.001$ ($n = 11$ [cell number], mean ± S.E.). Statistical analyses were assessed using Student's *t* test. Quantification data are shown in Supplemental Data 2.

immunostaining in the cell body was not reduced by the expression of shRNA against Alcα, despite significantly decreased Alcα expression in the cell body (Figure 3B). In these neurons, Fzd5 expression in axons was detected by immunostaining and then quantified (Figure 3C). Fzd5 immunoreactivity was significantly lower in the axons of neurons ($p < 0.001$; Figure 3C, right graph) in which the expression of Alcα was decreased compared with mock-treated neurons (Figure 3A). Although we cannot rule out a possibility of an off-target effect, these results suggest a substantial contribution of Alcα for the anterograde-axonal transport of Fzd5. These results indicate that Fzd5 is preferentially transported in Alcα-containing vesicles via kinesin-1 in axons, but the transport of Fzd5 by Alcα may be not exclusive in the immature neurons.

Fzd5 is predominantly transported at the velocity of Alcα transport vesicles rather than that of APP transport vesicles

To examine that Alcα-containing vesicles preferentially transport Fzd5 in axons, we performed the velocity analysis of transport vesicles by overexpressing Fzd5-EGFP in primary cultured neurons. In WT neurons, APP vesicles are transported faster than Alcα-harboring vesicles. This higher velocity of fast axonal transport for APP vesicles is designated as the EFV and mediated via JIP1b that connects APP to kinesin-1 (Araki *et al.*, 2007; Chiba *et al.*, 2014a; Chiba *et al.*, 2017; Tsukamoto *et al.*, 2018). Using this property, we analyzed the transport velocity of Fzd5 in axons. Fzd5-EGFP was expressed in mouse primary-cultured neurons, together with Alcα-EGFP and APP-EGFP. The velocity of EGFP-proteins for anterograde transport was analyzed with TIRF microscopy (Figure 4; Supplemental Movies 1–3). As previously reported, the average velocity of Alcα anterograde transport (1.66 ± 0.49 μm/s) is similar to that of kinesin-1 moving along microtubules, calculated in vitro at 35°C (Kawaguchi and Ishiwata, 2000), while the average velocity of APP (2.90 ± 0.71 μm/s) was of the EFV (Figure 4A and B). The average velocity of Fzd5 (2.26 ± 0.82 μm/s) was intermediate between the average values for Alcα and APP. This may be due to the fact that Fzd5 is a cargo content, which can be transported by using various cargo receptors. In line with this, the velocity distribution of Fzd5 was far from Gaussian. However, the first peak velocity (closed arrowhead at 1.6–1.8 μm/s) fits with the speed of Alcα transport (compare panels A to C) and is separate from the point of average velocity (open arrowhead; Figure 4C). The second peak with the velocity of 2.6–2.8 μm/s (gray arrowhead) correlated with the velocity of APP transport (compare panels B and C). These results suggest that the velocity of Fzd5 transport in the axon is composed of at least two velocities: 1) the major component mediated by Alcα (closed arrowhead) and, 2) the minor component by APP (gray arrowhead) vesicles. Although we cannot rule out possibilities that other unidentified cargo receptors of kinesin-1 and/or other kinesin motors may be joining the anterograde transport of Fzd5 with various velocities, the velocity analysis suggests that Fzd5 is transported with Alcα-containing vesicles more frequently than with APP-containing vesicles that show EFV in axons.

Localization and possible function of Fzd5 in axonal terminals by Alcα in adult brains

Anterograde transport of Fzd5 by either Alcα or APP transport vesicle predicts the localization of Fzd5 in axonal terminals. We examined whether Fzd5 transported to nerve terminals of mature neurons may be relevant for biological functions. We analyzed Fzd5 in a synaptosomal fraction prepared from the brains of adult Alcα-KO, APP-KO, and WT mice (Figure 5). The levels of Fzd5 in brain lysate from Alcα-KO and APP-KO mice were similar to that in WT mice (Figure 5A). However, Fzd5 levels in the synaptosomal fraction of both Alcα-KO and APP-KO mice were significantly ($p < 0.05$) reduced and amounted only to 70–80% of WT level (Figure 5B), suggesting that both Alcα- and APP-containing vesicles contribute to the transport of Fzd5 into nerve terminals in mature neurons in vivo.

A decrease in Fzd5 levels in nerve terminals may influence Wnt signaling in Alcα-KO and APP-KO mice brains. Three Wnt signaling pathways are known. The canonical pathway causes β-catenin accumulation, whereas one noncanonical pathway activates JNK, and the second activates CaMKII (Inestrosa and Varela-Nallar, 2015). To determine which Wnt signaling pathway may be affected by the Alcα– or APP-mediated transport of Fzd5, we analyzed the expression of intracellular-signaling molecules using immunoblotting (Figure 5, C–H). In total brain lysate and the synaptosomal fraction, β-catenin levels were unchanged between mutant and WT mice (Figure 5, C and D). This suggested that the canonical Wnt signaling pathway in nerve terminals was not regulated by Alcα- and APP-mediated transport of Fzd5. Phosphorylation levels of JNK p54 but not p45 tended to increase in brain lysates from Alcα-KO and APP-KO mice (Figure 5E), suggesting the possible activation of p54 JNK. However, this tendency of JNK, p54 and p46 activation was not observed in the synaptosomal fraction (Figure 5F), indicating that the JNK signaling pathway may be independent of the axonal transport of Fzd5. Finally, we examined a possible activation of CaMKII in nerve terminals (Figure 5, G and H). As a baseline, we determined the levels of phosphorylated CaMKII in total brain lysates of mutants and WT mice (Figure 5G). No significant differences were detectable. However, the abundance of phosphorylated CaMKII decreased significantly in the synaptosomal fraction from Alcα-KO mice ($p < 0.05$) and also showed a trend towards a decrease in APP-KO mice (Figure 5H), indicating that CaMKII activation was reduced in nerve terminals in the Alcα-KO mouse brain. This finding may be consistent with data showing the preferential transport of Fzd5 into nerve terminals by Alcα-containing vesicles. Taken together, Alcα and also APP may contribute to regulating the Ca^{2+}-dependent noncanonical Wnt signaling pathways in nerve terminals by mediating the anterograde transport of the Wnt receptor Fzd5 in mature neurons of the adult-mouse brain (Figure 6).

DISCUSSION

In this study, we provide biochemical evidence that Fzd5 is contained predominantly in Alcα-containing vesicles of adult-mouse brains. We also showed that, in axons of primary cultured neurons derived from embryonic brains that express smaller amounts of Fzd5 than adult-mouse brains, Fzd5 is transported preferentially with Alcα- containing vesicles rather than APP-containing vesicles. Alcα and APP serve as cargo receptors of membrane-transport vesicles via association with kinesin-1 (Konecna *et al.*, 2006; Araki *et al.*, 2007; Kawano *et al.*, 2012), thus, the reduced Fzd5 transport to the nerve terminals by the depletion of Alcα vesicles may lead to a decrease in noncanonical Wnt signaling. This suggests that cargo receptors may play an important role for anterograde transport of signaling molecules to nerve terminals.

Kinesin-1 plays an important role in the anterograde transport of membrane vesicles and organelles in the neuronal axon (Verhey and Hammond, 2009). Previous observations suggest that Alcα- and APP-transport vesicles are differentially regulated in axons, particularly in their differential velocities, although they use the same kinesin-1 motor (Araki *et al.*, 2007; Ludwig *et al.*, 2009; Kawano *et al.*, 2012; Vagnoni *et al.*, 2012; Chiba *et al.*, 2014a; Chiba *et al.*, 2017). Furthermore, approximately only 30% of the transporting vesicles contain both proteins in axons of mature neurons (Araki *et al.*, 2007), but do compensate for self-transport if one of the cargo receptors is

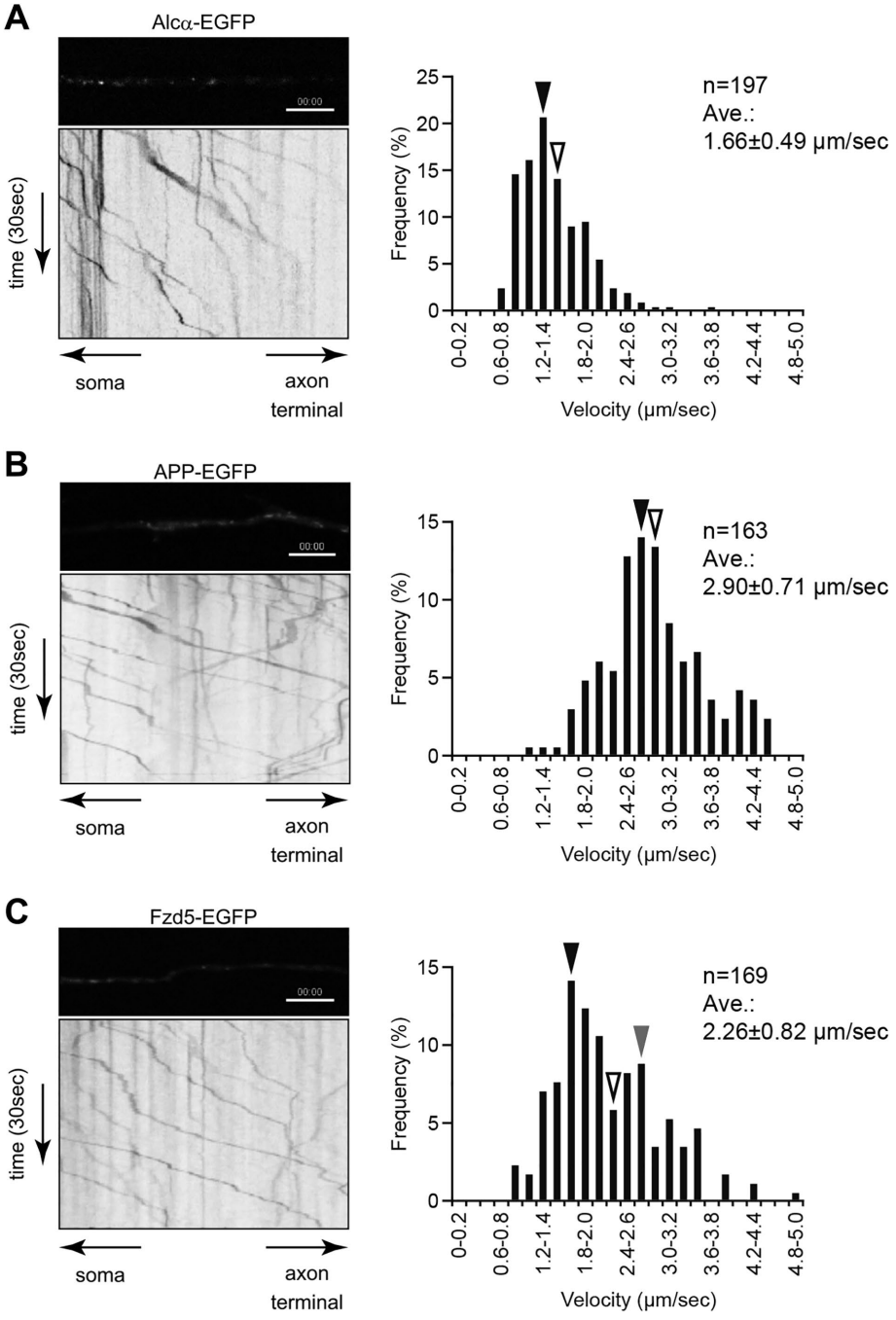

FIGURE 4: Anterograde transport velocity of Fzd5 in the neuronal axon. Anterograde transport velocity of Fzd5 was examined in mouse primary cultured neurons. Alcα-EGFP (A), APP-EGFP (B), and Fzd5-EGFP (C) were expressed in mouse neurons, and their transport was analyzed. Movies (see Supplemental Movies 1–3) and kymographs are shown on the left-hand side. Scale bar, 5 μm. The cumulative frequencies of velocities of anterograde transport of Alcα, APP, and Fzd5 are shown on the right. Average velocity is indicated with an open arrowhead, and most frequent velocity is indicated with a closed arrowhead. A gray arrowhead in panel C indicates the second peak with a velocity.

unable to bind to kinesin-1 (Sobu *et al.*, 2017). These distinctive properties of both transport-membrane vesicles suggest that Alcα vesicles may transport characteristic cargo proteins that are distinct from APP vesicles. Although one study suggests that Alcα/Clstn1 is involved in the axonal-transport of endosomal vesicles (Steuble *et al.*, 2010), it remained unclear as to what content is transported into nerve terminals by Alcα- and/or APP-transport vesicles, respectively.

As expected, our biochemical analysis of the cargo proteins within Alcα- and APP-transport vesicles revealed that Alcα- and APP-harboring vesicles, which were derived from the brains of adult mice, include specific and/or distinct proteins. Among the detected proteins in five independent analyses, 76–80% of proteins were characteristic for either Alcα- (140/176) or APP (114/150)-containing vesicles, whereas 20–24% of proteins were common in both transport vesicles (listed in Supplemental Tables S1–3 and summarized in Figure 1C). Many of these ubiquitous proteins are related to membrane-trafficking proteins rather than cargo proteins. We showed in part that Alcα- and APP-containing vesicles are likely to be functionally independent through the transport of different molecules into nerve terminals. Transport deficiency of various cargo proteins into the nerve terminals by the functional disturbance of cargo receptors such as Alcα and APP may generate aberrant neuronal phenotypes that are similar to the phenotypes of animals deficient for these cargo proteins (Wang *et al.*, 2005; Korte *et al.*, 2012; Ortiz-Medina *et al.*, 2015; Alther *et al.*, 2016).

Among cargo proteins, we focused on Fzd5, a molecule characteristic of Alcα vesicles in adult-mouse brains with biochemical analysis. Fzds act at nerve terminals as receptors of the Wnt signaling pathway and establish neuronal polarity (reviewed in Inestrosa and Varela-Nallar, 2015). We discovered that Fzd5 was present in Alcα-containing transport vesicles based on the following five findings: 1) Alcα vesicles isolated from adult-mouse brains with an Alcα-specific antibody contained Fzd5, 2) immunoisolation of vesicles with an anti-KHC antibody recovered Fzd5 with cargo receptors Alcα and APP, 3) Fzd5 colocalized preferentially with Alcα rather than with APP in axons of differentiating neurons although the expression of Fzd5 was low in the immature neurons, 4) reduction of Alcα, but not APP, expression decreased Fzd5 distribution in the axon, and 5) Alcα-KO mice showed significantly lower Fzd5 expression in synaptosomal fractions than WT mice. Our analysis showed that Fzd5 was more abundant in Alcα- than in APP-harboring vesicles, especially in adult-mouse brains. This is well in line with our in vitro observation that the distribution of Fzd5 transport velocity is likely to be a combined distribution composed of Alcα velocity and APP velocity, although we cannot rule out the possibility that transport vesicles harboring other cargo receptors may contribute to the anterograde transport Fzd5 in immature neurons.

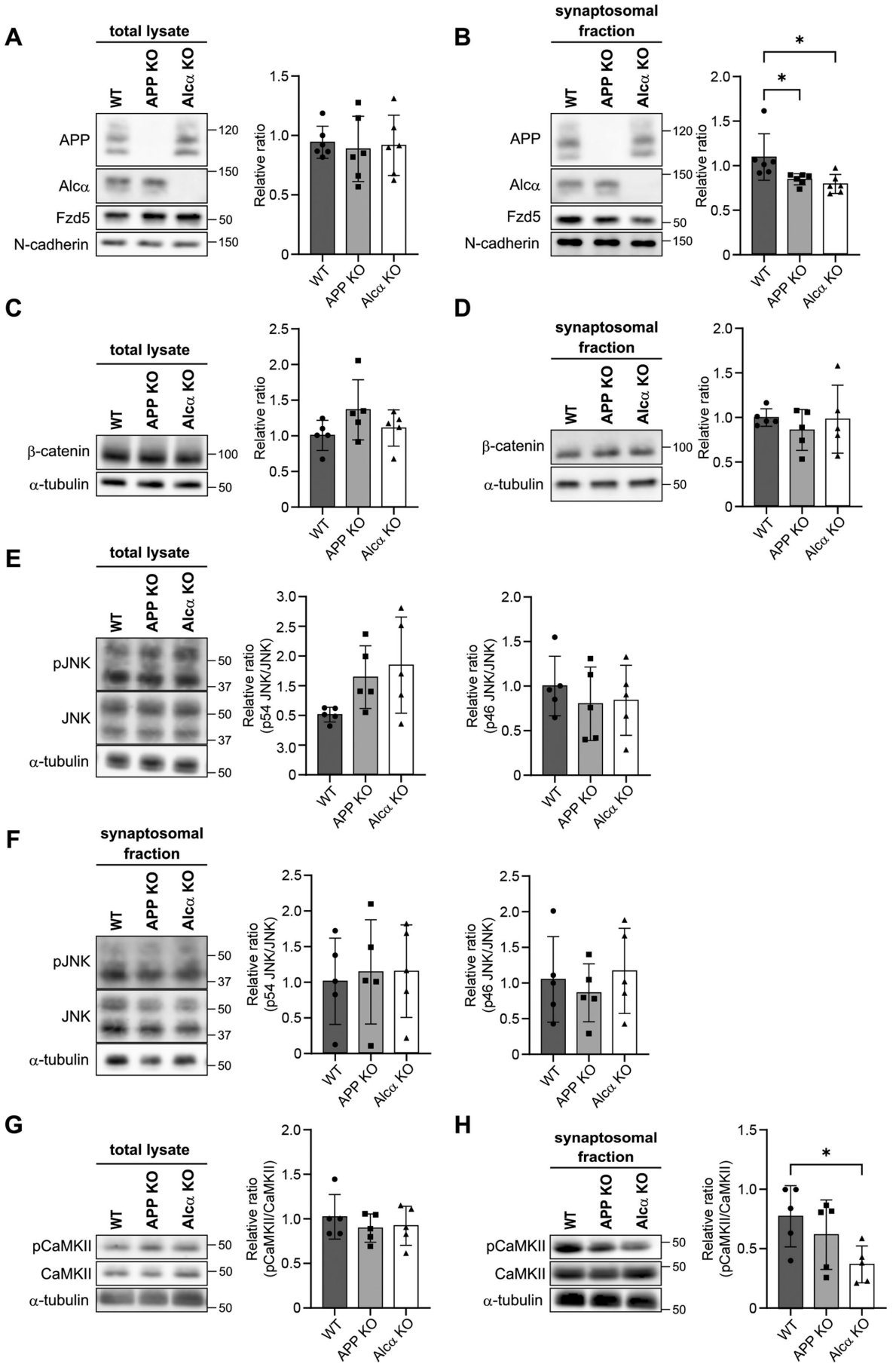
A
total lysate
WT
APP KO
Alcα KO
APP
Alcα
Fzd5
N-cadherin
120
150
50
150
Relative ratio
1.5
1.0
0.5
0
WT
APP KO
Alcα KO
B
synaptosomal fraction
WT
APP KO
Alcα KO
APP
Alcα
Fzd5
N-cadherin
120
150
50
150
*
*
Relative ratio
2.0
1.5
1.0
0.5
0
WT
APP KO
Alcα KO
C
total lysate
WT
APP KO
Alcα KO
β-catenin
α-tubulin
100
50
Relative ratio
2.5
2.0
1.5
1.0
0.5
0
WT
APP KO
Alcα KO
D
synaptosomal fraction
WT
APP KO
Alcα KO
β-catenin
α-tubulin
100
50
Relative ratio
2.0
1.5
1.0
0.5
0
WT
APP KO
Alcα KO
E
total lysate
WT
APP KO
Alcα KO
pJNK
JNK
α-tubulin
50
37
50
37
50
Relative ratio (p54 JNK/JNK)
3.0
2.5
2.0
1.5
1.0
0.5
3.0
0
WT
APP KO
Alcα KO
Relative ratio (p46 JNK/JNK)
2.0
1.5
1.0
0.5
0
WT
APP KO
Alcα KO
F
synaptosomal fraction
WT
APP KO
Alcα KO
pJNK
JNK
α-tubulin
50
37
50
37
50
Relative ratio (p54 JNK/JNK)
2.5
2.0
1.5
1.0
0.5
0
WT
APP KO
Alcα KO
Relative ratio (p46 JNK/JNK)
2.5
2.0
1.5
1.0
0.5
0
WT
APP KO
Alcα KO
G
total lysate
WT
APP KO
Alcα KO
pCaMKII
CaMKII
α-tubulin
50
50
50
Relative ratio (pCaMKII/CaMKII)
2.0
1.5
1.0
0.5
0
WT
APP KO
Alcα KO
H
synaptosomal fraction
WT
APP KO
Alcα KO
pCaMKII
CaMKII
α-tubulin
50
50
50
*
Relative ratio (pCaMKII/CaMKII)
1.5
1.0
0.5
0
WT
APP KO
Alcα KO

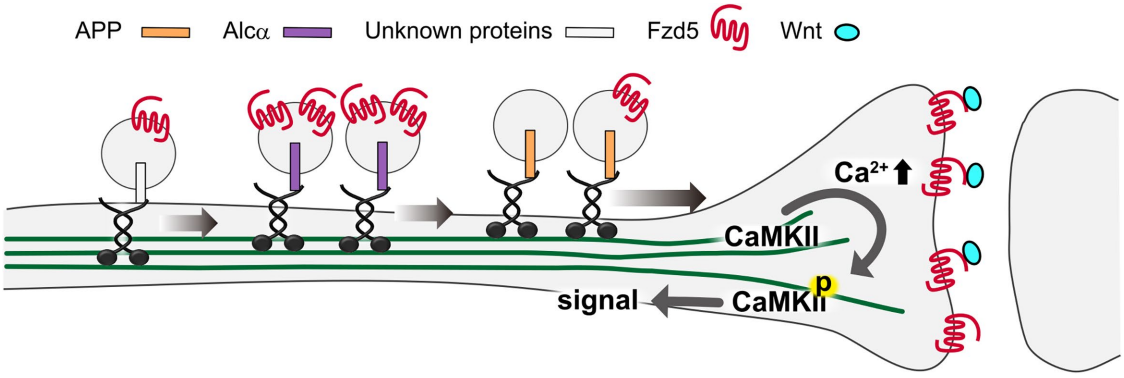

FIGURE 6: Schematic representation of Fzd5 localization by Alcα-containing transport vesicles in the axon and neuronal terminal of a mature neuron. In mature neurons, the axonal transport of Fzd5 is mostly performed with Alcα-containing transport vesicles, whereas APP-harboring vesicles contribute moderately to Fzd5 transport. Unknown/unidentified cargo receptor may also take part in the transport of Fzd5. Fzd5 is believed to localize mostly on the plasma membrane of nerve terminals. Wnt proteins bind to Fzd5 and may activate the Ca^{2+}-dependent noncanonical-signaling pathway, through which CaMKII may be phosphorylated and activated to facilitate cellular-signal transduction. Compared to WT mice, Wnt-mediated CaMKII signaling is impaired in the synaptosomes of Alcα-KO mice.

Fzd5 is reported to express at developmental stages coinciding with synaptogenesis and is involved in morphogenesis and the formation of neuron polarity (Sahores *et al.*, 2010; Slater *et al.*, 2013). Alcα/Clstn1 mediates the trafficking of Fzd3 that is involved in the regulation of axonal guidance (Alther *et al.*, 2016), although the underlying molecular mechanisms are unclear. Because the axonal-anterograde transport system plays an important role in neuronal-maturation processes such as polarity formation and in neuronal functions at nerve terminals, the deficiency of cargo receptors such as Alcα and APP in the transport vesicles may cause insufficient-neuronal maturation or disordered-neuronal functions in mature neurons via the lack of transport of crucial-cargo proteins. Our analyses using Alcα- and APP-KO mice show that Fzd5, transported by major Alcα- and minor APP- transport vesicles at the nerve terminus, may contribute to the Ca^{2+}-dependent noncanonical Wnt signaling pathway involved in CaMKII activation but not the activation of the canonical β-catenin pathway (Figure 6). Cargo receptors of kinesin motor such as Alcα and APP may thus contribute to the regulation of Fzd5-mediated Wnt signaling in nerve terminals of mature neurons. Further work is needed to substantiate this hypothesis. The present study highlights the importance of cargo-receptor function in linking-membrane vesicles containing various content to molecular-motor proteins. Further functional analysis of cargo receptors including Alcα and APP should shed light on the molecular mechanisms of neural development and functions.

MATERIALS AND METHODS

APP -KO and Alcα-KO mice

APP-KO mice (Li *et al.*, 1996) and Alcadein α (Alcα)/Calsyntenin 1 -KO (B6NJcl,Cg-Clstn1<tm1.1Tymo>, RRID:IMSR_RBRC11513) mice (Gotoh *et al.*, 2020) were used in this study with WT C57BL/6J mice (RRID 000664; Charles River Laboratories Japan, Yokohama, Japan). All mice were housed in a specific pathogen-free environment with a microenvironment vent system (Allentown Inc., Allentown, NJ, USA), under a 12-h light and dark cycle with free access to food and water. Male or female siblings (3–5) were housed per cage (floor space, 535 cm^2) with a micro barrier top. All animal studies were conducted in compliance with the ARRIVE guidelines, and all experimental protocols were approved by the Animal Care and Use Committees of Hokkaido University.

Preparation of transport-membrane vesicle fractions by size-fractionation

Transport-membrane vesicles were prepared using a modified version of the method previously reported (Steuble *et al.*, 2010). Briefly, the cerebral cortex from 2–3-mo-old C57BL/6 WT mice was homogenized 10 times on ice with a Dounce glass homogenizer in 3 ml of buffer A (5 mM HEPES-NaOH (pH 7.6), 320 mM sucrose, and 1 mM EDTA) supplemented with a protease inhibitor (PI) cocktail (5 μg/mL chymostatin, 5 μg/mL leupeptin, and 5 μg/mL pepstatin). After centrifugation at 1000 × *g* for 10 min at 4°C, the nuclear precipitate (P1) and postnuclear supernatant (S1) were recovered. The S1 fraction was centrifuged at 11,000 × *g* for 10 min

FIGURE 5: Changes in Fzd5 and Wnt signaling proteins in nerve-terminal fractions in WT, Alcα-KO, and APP-KO mice brains. Crude lysates of the cerebral cortex (10 μg of protein) and its synaptosomal fraction (10 μg of protein) from WT, APP-KO, and Alcα-KO mice brains were used to analyze the levels of Fzd5 (A, B), β-catenin (C, D), JNK and pJNK (E, F), and CaMKII and pCaMKII (G, H) by immunoblotting, together with membrane (N-cadherin) and cytosolic protein (α-tubulin) markers. Protein levels were standardized with a marker protein, and the relative ratios are presented as bar graphs. In panels A–D, protein ratios were compared with the ratio in WT mice (given a value of 1.0). In panels E–H, the ratio of the amount of phosphorylated-protein kinase was compared with the total amount of protein kinase. Statistical significance was determined (means ± S.E., $n = 5$ [independent sample number]; $^*p < 0.05$). Statistical analyses were assessed using one-way ANOVAs combined with Tukey-Kramer post-hoc test and Dunnett's test for multiple comparisons.

at 4°C to obtain the S2 and the P2 fractions. The S2 fraction was further centrifuged at 40,000 × *g* for 40 min at 4°C to recover the P3 and the S3 fractions. The S3 fraction was then centrifuged at 166,000 × g for 60 min at 4°C to recover the P4 and S4 fractions. The P4 fraction, which largely contains transporting membrane vesicles that are ~50–200 nm in diameter (Supplemental Figure S1), was suspended in 100 µL of buffer A by rotation for 1 h at 4°C to prepare the transport-membrane vesicle fraction. The protein contents of the respective fractions were quantified with the microLowry protein assay (Fryer *et al.*, 1986), and 10 µg of protein/well was loaded for immunoblot analysis.

Synaptosomal preparation

The synaptosomal fraction was prepared using a modified version of the method previously described (Carlin *et al.*, 1980). The cerebral cortex from 1-mo-old C57BL/6 WT mice was homogenized 10 times on ice with a Dounce glass homogenizer in 3 ml of buffer A supplemented with PIs. After centrifugation at 1000 × g for 10 min at 4°C, the postnuclear supernatant (S1) was further centrifuged at 13,800 × *g* for 20 min at 4°C, and the precipitate (P2) was then recovered. The P2 fraction was suspended in 1 ml of buffer A and homogenized seven times in ice using a Dounce glass homogenizer (P2′ fraction). The P2′ fraction was layered in a tube with a discontinuous gradient containing 0.8-, 1.0-, and 1.2 M sucrose solutions in 5 mM HEPES-NaOH (pH 7.6) and centrifuged at 82,500 × *g* for 2 h at 4°C (Beckman-Coulter SW41Ti swing rotor, Pasadena, CA). The interphase (1 ml) between the 1.0 and 1.2 M sucrose solutions was collected as the synaptosomal fraction.

Immunoisolation of APP- and Alcα-containing membrane vesicles

To immunoisolate APP- and Alcα-containing vesicles, affinity-purified anti-APP (369) and anti-Alcα (UT195) IgG (6 µg) were preincubated with 60 µg of Dynabeads Protein G (Invitrogen, Carlsbad, CA) in 1 ml PBS (10 mM sodium phosphate [pH 7.6] and 150 mM NaCl) for 1 h at 4°C with rotation. The beads were washed twice in PBS and incubated with 500 µL of the transport membrane vesicle fraction (a suspended P4 fraction, 250 µg protein) for 2–4 h at 4°C with rotation. The beads were recovered, washed twice with PBS (500 µL), four times with PBS (100 µL), and resuspended in 10 µL of elution buffer 1 (5% wt/vol sodium deoxycholate [SDC] in 25 mM NH_4HCO_3 pH 8.0) for 5 min with agitation. The supernatant was collected, and the precipitate was further suspended in elution buffer 1. The second supernatant was collected, and the first and second supernatants were combined (20 µL, SDC eluate). The beads were further suspended twice in elution buffer 2 (5% wt/vol SDS in 25 mM NH_4HCO_3, pH8.0) for 5 min at room temperature, as described above, to recover the SDS eluate (20 µL). This two-step elution method has been described previously (Masuda *et al.*, 2008; Steuble *et al.*, 2010). Both the SDC and SDS eluates were analyzed by immunoblotting and/or LC-MS/MS analysis.

LC–MS/MS analysis of proteins associated with immunoisolated vesicles

After boiling the SDC eluate for 5 min, the sample was treated with 100 mM dithiothreitol in 25 mM NH_4HCO_3 (pH 8.0) for 30 min at 56°C, and with 55 mM iodoacetic acid in 25 mM NH_4HCO_3 (pH 8.0) for 20 min in the dark at room temperature. The sample was diluted in 0.5% SDC and digested in trypsin (0.5 µg) for 12 h at 37°C. SDC in the sample was removed with the aid of phase transfer surfactant (Masuda *et al.*, 2008), and the sample was filtered (0.20-µm pore size) and concentrated with a centrifugal concentrator.

The digested sample was first adsorbed to a nanoACQUITY UPLC Symmetry C18 Trap column (75 µm × 20 mm, Waters Co Ltd, Milford, MA), and the desalted and concentrated sample was then secondarily separated with an ACQUITY UPLC HSS T3 column (1.8 µm, 75 µm × 150 mm, Waters Co.). The samples were eluted with a 5–40% gradient of acetonitrile including 0.1% (vol/vol) formic acid for 80 min at 300 nL/min. Five independent experiments ($n = 5$) were performed. Respective MS analysis was performed with data-independent (MS^E) in a positive ion mode (source temperature, 120°C; capillary voltage, 3.0 kV). We identified proteins with PLGS (ProteinLynx Global SERVER Ver. 2.5) and used a mouse taxonomy database (Uniprot). The following search settings were used: Peptide Tolerance: Automatic; Fragment Tolerance: Automatic; Primary Digest Reagent: Trypsin; Fixed Modifications: Carbamidomethyl C; Variable Modifications: Acetyl K, Acetyl N-TERM, Deamidation, and Oxidation; Missed cleavages: one; False positive Rate: five. Accession numbers obtained from the PLGS analysis were converted to gene names using the Uniprot ID mapping tool, and duplicate gene names were excluded. Gene names identical to control samples were excluded from the results for APP- and Alcα-containing samples. Proteins identified at least once with a Protein Score greater than 200 were counted, and a Venn diagram was created.

Protein analysis

Proteins identified in either APP- or Alcα-containing vesicles were analyzed with the PANTHER system and classified (Thomas *et al.*, 2022) (http://www.pantherdb.org/panther/ontologies.jsp).

Primary culture of mouse neurons and plasmid transfection

Primary cultures of mixed mouse cortical and hippocampal neurons were prepared from embryonic day 15.5 mice as previously described (Chiba *et al.*, 2014a). Briefly, neurons were attached to a poly-L-lysine coated chamber (Nalgen Nunc in Thermo Fisher Scientific, Rochester, NY) at a density of 4×10^4 cells/cm^2 for immunostaining, or 8×10^4 cells/cm^2 for live imaging and expression knockdown analysis, and cultured in Neurobasal Medium (Life Technologies, Carlsbad, CA) supplemented with 2% B-27 (Invitrogen, Carlsbad, CA), 4 mM Glutamax I (Thermo Fisher Scientific), and 5% (vol/vol) heat-inactivated horse serum. Plasmid transfection of neurons was performed at DIV 3–4 with Lipofectamine 2000 (Thermo Fisher Scientific) for 8–16 h in preparation for total internal reflectance fluorescence (TIRF) microscopy analysis as described below, and for 24 h for the expression KD analysis.

Immunostaining of primary cultured neurons

Primary cultures of mixed-mouse cortical and hippocampal neurons (DIV 4–5) were fixed in 4% (wt/vol) paraformaldehyde in PBS for 10 min; permeabilized in 0.2% (vol/vol) Triton X-100 in PBS for 5 min; blocked in 1% (vol/vol) goat serum in PBS for 10 min; and incubated with anti-Fzd5, anti-Alcα (Col90), and anti-APP (22C11) antibodies in blocking solution at 4°C overnight. The neurons were washed and then incubated with secondary antibodies. Immunostained images were observed with fluorescence microscopy (BZ-X710, Keyence Co Ltd., Osaka, Japan) and analyzed with Image J (Fiji; Schindelin *et al.*, 2012). Fluorescence images were obtained with an all-in-one fluorescence microscope (BZ-X710, KEYENCE, Osaka, Japan) equipped with a Plan Apochromat 100× oil immersion objective (1.4 numerical aperture [NA], Nikon, Tokyo, Japan). One to three neurons were cultured within each well for immunostaining. Colocalization was calculated using Fiji/Image J and the Coloc2 Fiji plugin (ImageJ-Fiji-ImagLib; http://Fiji.sc or http://imageJ.net). Background, fluorescence intensity in the region of no

specific fluorescence in the vicinity of the target cell, was subtracted before analysis. The colocalization rates of Fzd5 with Alcα or APP were calculated from each frame of images (55.6 μm^2) of axon and are indicated as Pearson's *R*-value. Vesicles within two to three frames of the axon of a single cell were counted. All values were combined and subject to statistical analysis with the indicated cell numbers (*n*) as independent biological replicates. Quantification data were described in Supplemental Data 2.

TIRF microscopy analysis

Vesicular transport in living neuronal cells was observed with a TIRF microscopy system (C1; Nikon, Tokyo, Japan) and an oil immersion lens (Nikon CFI Apo TIRF [100 ×, NA = 1.49] in the incubation chamber [5% CO_2 at 37°C]). Images were recorded with a charge-coupled device camera Cascade 650 (Photometrics, Tucson, AZ) and analyzed with MetaMorph 6.1 software (Molecular Devices, San Jose, CA). Velocity was analyzed quantitatively as described (Chiba *et al.*, 2017), and the velocity of five frames at 200 ms/frame was averaged. A kymograph of moving vesicles in axons was assembled with KymoMaker (Chiba *et al.*, 2014b).

Plasmids

Mouse Fzd5 cDNA (585 amino acids, GeneBank accession number NM_022721) was prepared with cDNA derived from mRNA derived from the brains of 2-mo-old WT mice. The cDNA was amplified by PCR with forward (5′-GGGGTACCGCCACCAGGCTCGACCCGACCCGTC-3′) and reverse (5′-CCGCTCGAGTACGTGCGACAGGGACACTTGC-3′) primers. The product was purified and inserted into pcDND3.1 with a C-terminal EGFP sequence to generate pcDNA3.1-Fzd5-EGFP plasmid. pcDNA3.1-hAPP-EGF and pcDNA3.1-hAlcα-EGFP were previously described (Araki *et al.*, 2007). The pSuper-APP was designed to target nucleotides 1060–1078 (5′-AAGGCCGTTATCCAGCATT-3′) of mouse APP, and the pSuper-Alcα was generated to target nucleotides 1174–1192 (5′-GAGACAATTCTCTGCAGTT-3′) of mouse Alcα according to a previously described procedure (Nakaya *et al.*, 2008).

Antibodies

The anti-Alcα C-terminal guinea pig (Co190) and rabbit (UT195), anti-APP C-terminal rabbit (369), and anti-KLC1 rabbit (UT109) polyclonal antibodies have been described previously (Oishi *et al.*, 1997; Araki *et al.*, 2007; Maruta *et al.*, 2012; Sobu *et al.*, 2017). The anti-KIF5 mouse (H2) monoclonal antibody was provided by Dr. Bloom (Brady *et al.*, 1990; Pfister *et al.*, 1989). Anti-EEA1 (#610457, clone 14), anti-SYT (#610433, clone 41), Anti-MAP2B (#610460, clone 18), and anti-N-Cadherin (#610920, clone 32) mouse-monoclonal antibodies were purchased from BD Bioscience (Franklin Lakes, NJ). Anti-Rab1B (sc-599, G-20) rabbit-polyclonal antibody and anti-β-catenin (sc-7963, E-5), anti-SYP (sc-17750, D-4), and anti-VGAT (sc-393373, F-2) mouse-monoclonal antibodies were purchased from Santa Cruz Biotechnology (Dallas, TX). Anti-Rab7 (#9367, D95F2), anti-VAMP2 (#13508, D601A), antiphospho-SAPK/JNK (pThr183/pTyr185; #9255, G9), antiphospho-CamKII (pThr286; #12716, D21E4), and anti-Syntaxine 6 (#2417, C34B2) rabbit monoclonal and anti-SAPK/JNK (#9252) rabbit-polyclonal antibodies were purchased from Cell Signaling (Danvers, MA). Anti-APP N-terminal (22C11, CHEMICON, Temecula, CA), anti-α-tubulin (10G10, Wako, Osaka Japan), anti-Rab3C (N1C3, Genetex, Irvine, CA), anti-Rab11 (ERP787(B), Abcam, Cambridge, UK), anti-CaM kinase II (6G9, EMD Millipore, Burlington, MA), and anti-GFP (1E4, MBL, Tokyo Japan) mouse monoclonal antibodies, and anti-Rab10 (Bethyl Laboratories, Montgomery, TX), anti-VGlutT1 (ABN1647, Sigma-Aldrich, St Louise, MO), anti-Fzd5 (Y500, Bioworld Technology, Louis Park, MN), anti-Calnexin (Stressgen Biotech, San Diego, CA), and anti-actin (ABT1485, Merck Millipore, Burlington, MA) rabbit-polyclonal antibodies, were also purchased. The following secondary antibodies were used: Cy3-conjugated AffiniPure Donkey anti-Guinea Pig IgG (H+L; #706-165-148, Jackson ImmunoResearch Laboratories, West Grove, PA), Goat Anti-Rabbit IgG (H+L), Alexa Fluor 647 (ab150079, Abcam, Cambridge, UK), Goat anti-Mouse IgG (H+L), Alexa Fluor 488 (A-11001, Thermo Fisher Scientific, Waltham, MA).

Statistical analysis

Statistical differences were assessed using Student's *t* test or one-way ANOVA combined with the Tukey-Kramer post-hoc test and Dunnett's test for multiple comparisons (GraphPad Prism software, version 9.4.0). *P* values < 0.05 were considered significant.

ACKNOWLEDGMENTS

We thank Dr. Yoko Yamagata (National Institute for Physiological Sciences, Okazaki, Japan) for the reading and comments on the manuscript. This work was supported in part by the Strategic Research Program for Brain Sciences from the Japan Agency for Medical Research and Development (JP20dm0107142 to T.S.), The Naito Foundation (to S.H.), Pharmaceutical Research Grants of Takeda Science Foundation (to Y.S.), by KAKENHI, a Grants-in-Aid for Scientific Research (22K15270 to Y.S., 23K06840 to S.H.) from Japan Society for the Promotion of Science in Japan, and by a Grants-in-Aid for Scientific Research on Innovative Areas-Platform for Advanced Technologies and Research Resources "Advanced Bioimaging Support" to T.S.. Advanced Prevention and Research Laboratory for Dementia, Graduate School of Pharmaceutical Sciences, Hokkaido University is supported by Japan Medical Leaf co.

REFERENCES

Alther TA, Domanitskaya E, Stoeckli ET (2016). Calsyntenin 1-mediated trafficking of axon guidance receptors regulates the switch in axonal responsiveness at a choice point. Development 143, 994–1004.

Araki Y, Tomita S, Yamaguchi H, Miyagi N, Sumioka AKirino Y, Suzuki T (2003). Novel cadherin-related membrane proteins, Alcadeins, enhance the X11-like protein mediated stabilization of amyloid b-protein precursor metabolism. J Bio Chem 278, 49448–49458.

Araki Y, Miyagi N, Kato N, Yoshida T, Wada S, Nishimura M, Komano H, Yamamoto T, De Strooper B, Yamamoto K, Suzuki T (2004). Coordinated metabolism of Alcadein and amyloid β-protein precursor regulates FE65-dependent gene transactivation. J Bio Chem 279, 24343–24354.

Araki Y, Kawano T, Taru H, Saito Y, Wada S, Miyamoto K, Kobayashi H, Ishikawa HO, Oshsugi Y, Yamamoto T, *et al.* (2007). The novel cargo Alcadein induces vesicle association of kinesin-1 motor components and activates axonal transport. EMBO J 26, 1475–1486.

Benilova I, Karran E, De Strooper B (2012). The toxic Aβ oligomer and Alzheimer's disease: an emperor in need of clothes. Nat Neurosci 15, 349–357.

Brady ST, Pfister KK, Bloom GS (1990). A monoclonal antibody against kinesin inhibits both anterograde and retrograde fast axonal transport in squid axoplasm. Proc Natl Acad Sci USA 87, 1061–1065.

Carlin RK, Grab DJ, Cohen RS, Siekevitz P (1980). Isolation and characterization of postsynaptic densities from various brain regions: Enrichment of different types of postsynaptic densities. J Cell Biol 86, 831–843.

Chiba K, Araseki M, Nozawa K, Furukori K, Araki Y, Matsushima T, Nakaya T, Hata S, Saito Y, Uchida S, *et al.* (2014a). Quantitative analysis of APP axonal transport in neurons – Role of JIP1 in APP anterograde transport. Mol Biol Cell 25, 3569–3580.

Chiba K, Shimada Y, Kinjo M, Suzuki T, Uchida S (2014b). Simple and direct assembly of kymographs from movies with Kymomaker. Traffic 15, 1–11.

Chiba K, Chien K-y, Sobu Y, Hata S, Kato S, Nakaya T, Okada Y, Nairn AC, Kinjo M, Taru H, *et al.* (2017). Phosphorylation of KLC1 modifies interaction with JIP1 and abolishes the increased fast velocity of APP transport by kinesin-1. Mol Biol Cell 28, 3857–3869.

Dodding MP, Mitter R, Humphries AC, Way M (2011). A kinesin-1 binding motif in vaccinia virus that is widespread throughout the human genome. EMBO J 30, 4523–4538.
Fryer HJL, Davis GE, Manthorpe M, Varon S (1986). Lowry protein assay using an automatic microtiter plate spectrophotometer. Anal Biochem 153, 262–266.
Galanis C, Fellenz M, Becker D, Bold C, Lichtenthaler SF, Müller UC, Deller T, Vlachos A (2021) Amyloid-β mediates homeostatic synaptic plasticity. J Neurosci 41, 5157–5172.
Gandy S (2023). Systemically administered alcadin peptide p3-Alcβ neutralizes brain Alzheimer's Aβ oligomers. Trends Mol. Med. 29, 487–488.
Goto N, Saito Y, Hata S, Saito H, Oima D, Murayama C, Shigeta M, Abe T, Konno D, Matsuzaki F, *et al*. (2020). Amyloidogenic processing of amyloid β protein precursor (APP) is enhanced in the brains of Alcadein α-deficient mice. J Biol Chem 295, 9650–9662.
Hata S, Fujishige S, Araki Y, Kato N, Araseki M, Nishimura M, Hartmann D, Saftig P, Fahrenholz F, Taniguchi M, *et al*. (2009). Alcadein cleavages by APP α- and γ-secretases generate small peptides p3-Alcs indicating Alzheimer disease-related γ-secretase dysfunction. J Biol Chem 284, 36024–36033.
Hata S, Fujishige S, Araki Y, Taniguchi M, Urakami K, Peskind E, Akatsu H, Araseki M, Yamamoto K, Martins RN, *et al*. (2011). Alternative processing of γ-secretase substrates in common forms of mild cognitive impairment and Alzheimer's disease: evidence for γ-secretase dysfunction. Ann Neurol 69, 1026–1031.
Hata S, Omori C, Kimura A, Saito H, Kimura N, Gupta V, Pedrini S, Hone E, Chatterjee P, Taddei K, *et al*. (2019). Decrease in p3-Alcβ37 and p3-Alcβ40, products of Alcadein β generated by γ-secretase cleavages, in aged monkeys and patients with Alzheimer's disease. Alzheimers Dement (NY) 5, 740–750.
Hata S, Saito H, Kakiuchi T, Fukumoto D, Yamamoto S, Kasuga K, Kimura A, Moteki K, Abe R, Adachi S, *et al*. (2023) Brain p3-Alcβ peptide restores neuronal viability impaired by Alzheimer's amyloid β-peptide. EMBO Mol Med 15, e17052.
Hintsch G, Zurlinden A, Meskenaite V, Steuble M, Fink-Widmer K, Kinter J, Sonderegger P (2002). The calsyntenins a family of postsynaptic membrane proteins with distinct neuronal expression patterns. Mol Cell Neurosci 21, 393–409.
Inestrosa NC, Varela-Nallar L (2015). Wnt signaling in neuronal differentiation and development. Cell Tissue Res 359, 215–223.
Kamal A, Stokin GB, Yang Z, Xia CH, Goldstein LS (2000). Axonal transport of amyloid precursor protein is mediated by direct binding to the kinesin light chain subunit of kinesin-I. Neuron 28, 449–459.
Kawaguchi K, Ishiwata S (2000). Temperature dependent of force, velocity, and processivity of single kinesin molecules. Biochem Biophy Res Commun 272, 895–899.
Kawano T, Araseki M, Araki Y, Kinjo M, Yamamoto T, Suzuki T (2012). A small peptide sequence is sufficient for initiating kinesin-1 activation through part of TPR region of KLC1. Traffic 13, 834–848.
Kjos I, Vestre K, Guadagno NA, Distefano MB, Progida C (2018). Rab and Arf proteins at the crossroad between membrane transport and cytoskeleton dynamics. Biochim Biophys Acta Mol Cell Res 1865, 1397–1409.
Kondo M, Shiono M, Itoh G, Takei N, Matsushima T, Maeda M, Taru H, Hata S, Yamamoto T, Saito Y, Suzuki T (2010). Increased amyloidogenic processing of transgenic human APP in X11-like deficient mouse brain. Mol Neurodegener 5, 35.
Konecna A, Frischnech R, Kinter J, Ludwig A, Steuble M, Meskenaite V, Indermuhle M, Engrl M, Cen C, Mateos JM, *et al*. (2006). Calsyntenin-1 docks vesicular cargo to kinesin-1. Mol Biol Cell 17, 3651–3663.
Korte M, Herrmann U, Zhang X, Draguhn A (2012). The role of APP and APLP for synaptic transmission, plasticity, and network function: lessons from genetic mouse models. Exp. Brain Res. 217, 435–440.
Li Z-W, Stark G, Gotz J, Rülicke T, Müller U, Weissmann C (1996). Generation of mice with a 200-kb amyloid precursor protein gene deletion by Cre recombinase-mediated site-specific recombination in embryonic stem cells. Proc Natl Acad Sci USA 93, 6158–6162.
Ludwig A, Blume J, Diep TM, Yuan J, Mateos JM, Leuthauser K, Steuble M, Streit P, Sonderegger P (2009). Calsyntenins mediate TGN exit of APP in a kinesin-1-dependent manner. Traffic 10, 572–589.
Masuda T, Tomita M, Ishihama Y (2008). Phase transfer surfactant-aided trypsin digestion for membrane proteome analysis. J. Proteome Res. 7, 731–740.
Mehr A, Hick M, Ludewig S, Müller M, Herrmann U, von Egelhardt J, Wolfer D, Korte M, Müller UC (2020). Lack of APP and APLP2 in GABAergic forebrain neurons impairs synaptic plasticity and cognition. Cereb Cortex 30, 4044–4063.
Maruta C, Saito Y, Hata S, Gotoh N, Suzuki T, Yamamoto T (2012). Constitutive cleavage of the single-pass transmembrane protein Alcadeinα prevents aberrant peripheral retention of kinesin-1. PLoS One 7, e43058.
Motodate R, Saito Y, Hata S, Suzuki T (2016). Expression and localization of X11 family proteins in neurons. Brain Res 1646, 227–234.
Mucke L, Selkoe DJ (2012). Neurotoxicity of amyloid β-protein: synaptic and network dysfunction. Cold Spring Harb Perspect Med 2, a006338.
Müller UC, Deller T, Korte M (2017). Not just amyloid: physiological function of the amyloid precursor protein family. Nat Rev Neurosci 18, 281–298.
Nakaya T, Kawai T, Suzuki T (2008). Regulation of FE65 nuclear translocation and function by amyloid β-protein precursor in osmotically stressed cells. J Biol Chem 283, 19119–19131.
Oishi M, Nairn AC, Czernik AJ, Lim GS, Isohara T, Gandy SE, Greengard P, Suzuki T (1997). The cytoplasmic domain of the Alzheimer's β-amyloid precursor protein is phosphorylated at Thr654, Ser655 and Thr668 in adult rat brain and cultured cells. Mol Med 3, 111–123. PMCID: PMC2230054
Omori C, Kaneko M, Nakajima E, Akatsu H, Waragai M, Maeda M, Morishima-Kawashima M, Saito Y, Nakaya T, Taru H, *et al*. (2014) Increased levels of plasma p3-Alcα35, a major fragment of Alcadeinα by γ-secretase cleavage, in Alzheimer's disease. J Alzheimers Dis 39, 861–870.
Ortiz-Medina H, Emond MR, Jontes JD (2015). Zebrafish calsyntenins mediate hemophilic adhesion through their amino-terminal cadherin repeats. Neuroscience 286, 87–96.
Pfister KK, Wagner MC, Stenoien DL, Brady ST, Bloom GS (1989). Monoclonal antibodies to kinesin heavy and light chains stain vesicle-like structures, but not microtubules, in cultured cells. J Cell Biol 108, 1453–1463.
Piao Y, Kimura A, Urano S, Saito Y, Taru H, Yamamoto T, Hata S, Suzuki T (2013). Mechanism of intramembrane cleavage of Alcadeins by γ-secretase. PLoS One 8, e62431.
Richter M, Ludewig S, Winschel A, Abel T, Bold C, Salzburger LR, Klein S, Han K, Weyer SW, Fritz A-K, *et al*. (2018). Distinct in vivo roles of secreted APP ectodomain variants APPsα and APPsβ in regulation of soine density, synaptic plasticity, and cognition. EMBO J 37, e98335.
Sahores M, Gibb A, Salinas P (2010). Frizzled-5, a receptor for the synaptic organizer Wnt7a, regulates activity-mediated synaptogenesis. Development 137, 2215–2225.
Schindelin J, Arganda-Carreras I, Frise E, Kaynig V, Longair M, Pietzsch T, Preibisch S, Rueden C, Saalfeld S, Schmid B, *et al*. (2012) Fiji: An open-source platform for biological-image analysis. Nat Methods 9, 676–682.
Slater PG, Ramirez VT, Gonzalez-Billault C, Varela-Nallar L, Inestrosa NC (2013). Frizzled-5 receptor is involved in neuronal polarity and morphogenesis of hippocampal neurons. PLoS ONE 8, e78892.
Sobu Y, Furukori K, Chiba K, Nairn AC, Kinjyo M, Hata S, Suzuki T (2017). Phosphorylation of multiple sites within an acidic region of Alcadein α is required for kinesin-1 association and Golgi exit of Alcadein α cargo. Mol Biol Cell 28, 3844–3856.
Steuble M, Gerrits B, Ludwig A, Mateos JM, Diep T-M, Tagaya M, Stephan A, Schatzle P, Kunz B, Streit P, Sonderegger P (2010). Molecular characterization of a trafficking organelle: Dissecting the axonal paths of calsyntenin-1 transport vesicles. Proteomics 10, 3775–3788.
Steubler V, Erdinger S, Back MK, Ludewig S, Fassler D, Richter M, Han K, Slomianka L, Amrein I, von Engelhardt J, *et al*. (2021). Loss of all three APP family members during development impairs synaptic function and plasticity, disrupts learning, and cause an autism-like phenotype. EMBO J 40, e107471.
Suzuki T, Nakaya T (2008). Regulation of amyloid beta-protein precursor by phosphorylation and protein interactions. J Biol Chem 283, 29633–29637.
Szodorai A, Kuan Y-H, Hunzelmann S, Engel U, Sakane A, Sasaki T, Takai Y, Kirsch J, Müller UC, Beyreuther K, *et al*. (2009). APP anterograde transport reqires Rab3A GTPase activity for assembly of the transport vesicle. J. Neurosci. 29, 14534–14544.
Thomas PD, Ebert D, Muruganujan A, Mushayahama T, Albou L-P, Mi H (2022). PANTHER: Making genome-scale phylogenetics accessible to all. Protein Sci 31, 8–22.
Tsukamoto M, Chiba K, Sobu Y, Shiraki Y, Okumura Y, Hata S, Kitamura A, Nakaya T, Uchida S, Kinjo M, *et al*. (2018). The cytoplasmic region of the amyloid β-protein precursor (APP) is necessary and sufficient for the

enhanced fast velocity of APP transport by kinesin-1. FEBS Lett 592, 2716–2724.
Vagnoni A, Perkinton MS, Gray EH, Francis PT, Noble W, Miller CC (2012). Calsyntenin-1 mediates axonal transport of the amyloid precursor protein and regulates Aβ production. Hum Mol Genet 21, 2845–2854.
Vale RD, Reese T, Sheetz MP (1985). Identification of a novel force-generating protein, kinesin, involved in microtubule-based motility. Cell 42, 39–50.
Van der Kant R, Goldstein LSB (2015). Cellular functions of the amyloid precursor protein from development to dementia. Dev. Cell 32, 502–515.
Verhey KJ, Meyer D, Deehan R, Blenis J, Schnapp BJ, Rapoport TA, Margolis B (2001). Cargo of kinesin identified as JIP scaffolding proteins and associated signaling molecules. J Cell Biol 152, 959–970.
Verhey KJ, Hammond JW (2009). Traffic control: regulation of kinesin motors. Nat Rev Mol Cell Biol 10, 765–777.
Wang P, Yang G, Mosier DR, Chang P, Zaidi T, Gong Y-D, Zhao N-M, Dominguez B, Lee K-F, Gan W-B, Zheng H (2005). Defective neuromuscular synapses in mice lacking amyloid precursor protein (APP) and APP-like protein 2. J Neurosci 25, 1219–1225.
Yip YY, Permigo S, Sanger A, Xu M, Parsons M, Steiner RA, Dodding MP (2016). The light chains of kinesin-1 are autoinhibited. Proc Natl Acad Sci USA 113, 2418–2423.
Zhu H, Lee HY, Tong Y, Hong BS, Kim KP, Shen Y, Lim KJ, Mackenzie F, Tempel W, Park HW (2012). Crystal structures of the tetratricopeptide repeat domains of kinesin light chains: insight into cargo recognition mechanisms. PLoS One 7, e33943.